2011 IEEE International Conference on Robotics and Automation
Shanghai International Conference Center
May 9-13, 2011, Shanghai, China

A Torque Cancelling System Using the Parallel Solution Scheme

Daigoro Isobe, Yasumasa Matsui, and Kensuke Kondo

Abstract— **A new torque cancelling system (TCS) that stabilizes mechanical sway in quick-motion robots is discussed in this paper. It cancels the reaction moment generated by the motion of an object by considering the precise dynamics of the object and the body of the robot itself. The reaction moment can be obtained accurately using the parallel solution scheme of inverse dynamics, which handles the dynamics of complex robotic architectures by modeling them with finite elements. Once the reaction moment is known, it can be cancelled by applying an anti-torque to a torque generating device. In this paper, the general concepts of the TCS and the parallel solution scheme are first described. Then, some examples of torque cancelling due to accurate calculations of dynamics are demonstrated, by showing the experimental results carried out on a prototype TCS system. The objects used in the experiments include rigid and flexible, outboard and inboard links, where difficult assumptions are normally required to consider the accurate dynamics.**

I. Introduction

A new torque cancelling system that stabilizes mechanical sway in quick-motion robots is discussed in this paper. Mechanical sway generated by reaction moments occurring in the motion, for example, of space stations is a big issue that can not be neglected. Motion controls using the conservative law of angular momentum are applied by driving control momentum gyros (CMG) [1] or reaction wheels [2]. Applications of the gyros and the wheels are generally limited to slow momentum transitions, relying upon high-gain feedback control. Although the same strategy can be used in the motion control of robots when the momentum transitions are not so fast, the dynamics of the robots should be considered to effectively control quicker motions. The torque cancelling system (TCS) discussed in this paper cancels the reaction moment generated by the motion of an object by considering the precise dynamics of the object and the body of the robot itself. The reaction moment can be obtained accurately using a newly proposed solution scheme of inverse dynamics, which handles the dynamics of complex robotic architectures by modeling them with finite elements. Once the reaction moment is known, it can be cancelled by applying an anti-torque to a torque generating device.

The newly proposed solution scheme of inverse dynamics mentioned above is called the parallel solution scheme [3], and it was developed on the basis of a finite element approach. By taking advantage of the natural characteristics of the finite element method, i.e., the capability of expressing the behaviour of each discrete element as well as that of the entire continuous system, local information such as nodal forces and displacements can be calculated in parallel. In this scheme, the analyzed model is evaluated in absolute Cartesian coordinates with the equation of motion expressed in the dimension of force. The nodal forces are calculated incrementally in matrix form, which does not require any revision of the overall frame, and the variables forming the frame can be revised by simply changing the input data in the case of a physical change in the hardware system. The calculated nodal forces are then converted into joint torques using a matrix-form equation divided into terms of force, the transformation between the coordinates, and length. In contrast to the conventional and revised schemes that use dynamic equations [4]-[6], the structure of the algorithm makes it seamless in its application to different types of link system under various boundary conditions such as open- or closed-loop link systems. It can also consider the elasticity of constituted links or passive joints by only changing the input numerical model, without the need to revise any part of the scheme. Its validity in various feedforward control experiments of various kinds of link systems has been verified [7], [8].

In this paper, the general concept of the TCS is first described. Then, an outline of the inverse dynamics calculation scheme for handling accurate dynamics is shown, along with some examples of torque cancelling experiments carried out on a prototype TCS system. The objects used in the experiments include rigid and flexible, outboard and inboard links, where difficult assumptions are normally required to consider the accurate dynamics.

II. Torque Cancelling System

A robot swinging around an arm in a quick motion, for example, normally needs a counterbalance motion to avoid any mechanical sway. The TCS proposed in this paper is a system that generates anti-torque to suppress the mechanical sway, by computing accurate inverse dynamics of the arm motion with an accurate consideration of the dynamics of the

Manuscript received August 25, 2010.

D. Isobe is an associate professor of the Department of Engineering Mechanics and Energy, University of Tsukuba, Tsukuba-shi, Ibaraki 305-8573, Japan. e-mail: isobe@kz.tsukuba.ac.jp.

Y. Matsui is a master degree graduate student in the Department of Engineering Mechanics and Energy, University of Tsukuba, Tsukuba-shi, Ibaraki 305-8573, Japan. e-mail: e0712350@edu.esys.tsukuba.ac.jp.

K. Kondo is also a master degree graduate student in the Department of Engineering Mechanics and Energy, University of Tsukuba, Tsukuba-shi, Ibaraki 305-8573, Japan. e-mail: e0611350@edu.esys.tsukuba.ac.jp.

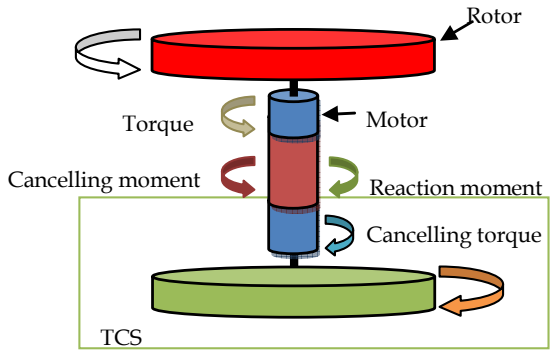

Fig. 1. General concept of uniaxial TCS.

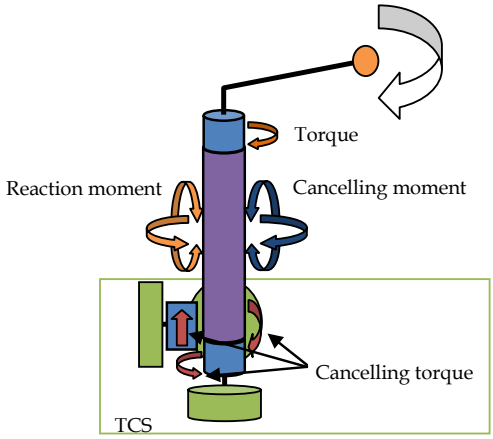

Fig. 2. General concept of triaxial TCS.

robot itself. The accurate consideration of the dynamics is carried out by implementing the parallel solution scheme which is to be explained briefly in the next section.

A simple explanation of the TCS is drawn in Fig. 1 for the uniaxial case. Suppose a rotor is rotated by a motor with a specific torque. A reaction moment will occur around the rotating axis which will make the whole body twist around the axis. To avoid the reaction moment from making the twist, a cancelling moment can be generated by another motor placed on the axis by supplying a specific, cancelling torque. The same concept is used in twin-rotator helicopters, where two rotators rotate in opposite directions to cancel the twist motion. However, the difference between the twin-rotator helicopters and the proposed TCS is that the TCS is driven using accurate torques by considering the dynamics related to the motion and the overall architecture, while the twin-rotators only rotate in opposite directions with the same rotational speed.

A general concept of triaxial TCS is drawn in Fig. 2. If an object in motion is considered as an outboard rotor (or a cantilever beam as shown in the figure), the reaction moments acting on the body become not as simple as those in the uniaxial case. The moments will act around three-dimensional axes because the center of gravity of the overall body is at the offset position from the rotating axis. To cancel these moments, three TCSs, each set on each dimensional axis, should be placed as shown in Fig. 2. However, all of the TCSs do not have to be placed at one place or placed exactly on the rotating axis, to maintain the function. Actually, a TCS can be mounted, literally, anywhere in the body. All a TCS has to do to suppress a mechanical sway is to cancel the moment generated at the precise location of the TCS.

III. Parallel Solution Scheme of Inverse Dynamics

In this section, an outline of the parallel solution scheme of inverse dynamics for considering accurate dynamics of the system is described. In the parallel solution scheme, a link system consisting of motor joints and links is modeled and subdivided using finite elements. A link is substituted with a single Bernoulli-Euler beam element, assuming a consistent mass distribution along the link [8]. The consistent mass matrix of a beam element is formulated in the same manner as the displacement function and does not require an expression of the center of gravity. This type of modeling has the merits of reducing computational time without lowering accuracy, particularly against elastic deformations. It requires only one-element subdivision per member for cases of infinitesimal deformation because the deformation of the element is defined using a high-order displacement function.

Figure 3 shows the nodal forces based on global coordinates acting on the i th link in a three-dimensional open-loop n-link system with a consistent mass distribution. The joint torque τ_{ix} required around the x-elemental axis on the i th link is determined by adding the $i+1$ th joint torque $\tau_{(i+1)x}$ to the sum of the moments of inertia acting on this link and is expressed by the nodal forces based on elemental (or link) coordinates as

$$\tau_{ix} = l_i(\sum_{j=i+1}^{n} F_j)_y + F_{i\phi x} + \tau_{(i+1)x}, \quad (i, j = 1 \sim n), \quad (1)$$

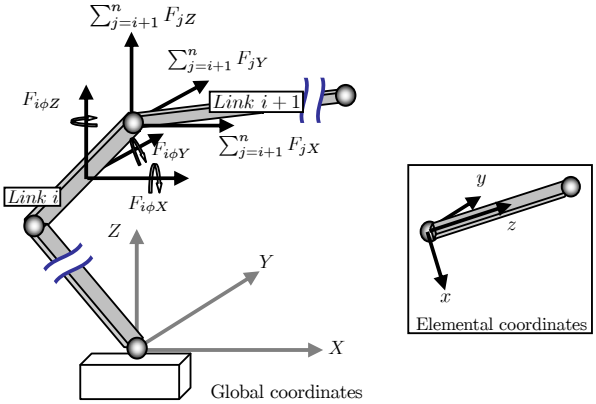

Fig. 3. Nodal forces acting on i th link in n-link system with consistent mass distribution.

where l is the link length and F is the nodal force. $(\sum F)$ indicates the resultant force, the subscripts i, j the link number, x, y, z the elemental coordinate components, X, Y, Z the global coordinate components, and φ the angular components. The right hand side of (1) becomes different in the scheme with a lumped mass distributed at the center of gravity [3]. By considering the other components around the y- and z-axes and arranging them into global coordinates (X, Y, Z) in matrix form, the joint torque vector is expressed as

$$\{\tau^n\} = [L^n][T^n]\{P^n\}, \tag{2}$$

where $\{P^n\}$ is a 6n×1 vector related to the nodal force and is defined as

$$\{P^n\} = \begin{Bmatrix} P_1 \\ P_2 \\ \cdot \\ \cdot \\ P_n \end{Bmatrix}, \quad where \quad \{P_i\} = \begin{Bmatrix} \sum_{j=i+1}^{n} F_{jX} \\ \sum_{j=i+1}^{n} F_{jY} \\ \sum_{j=i+1}^{n} F_{jZ} \\ F_{i\phi X} \\ F_{i\phi Y} \\ F_{i\phi Z} \end{Bmatrix}. \tag{3}$$

$[T^n]$ is a 6n×6n transformation matrix and is defined as

$$[T^n] = [h^n][T^n_{GE}], \tag{4}$$

where $[h^n]$ is a correction matrix between the x-y and z-x coordinate systems, which simply inverts the signs of the components in the y-axis direction. $[T^n_{GE}]$ is a transformation matrix between the global and elemental coordinates and is expressed as

$$\left[\ T^n_{GE}\ \right] = \begin{bmatrix} T_1 & & & & & \\ & T_2 & & & 0 & \\ & & T_3 & & & \\ & & & \cdot & & \\ & & & & \cdot & \\ & 0 & & & \cdot & \\ & & & & & T_n \end{bmatrix}, \tag{5}$$

where

$$\left[\ T_i\ \right] = \begin{bmatrix} A_i & 0 \\ 0 & A_i \end{bmatrix} \tag{6a}$$

and

$$\left[\ A_i\ \right] = \begin{bmatrix} cos\phi_{iXx} & cos\phi_{iYx} & cos\phi_{iZx} \\ cos\phi_{iXy} & cos\phi_{iYy} & cos\phi_{iZy} \\ cos\phi_{iXz} & cos\phi_{iYz} & cos\phi_{iZz} \end{bmatrix}, \tag{6b}$$

where φ_{iXx}, for example, represents the rotational angle between the X (global) and x (elemental) coordinates.

$[L^n]$ in (2) is a 3n×6n matrix related to link length and is expressed as

$$[L^n] = [T^n_\Lambda][\Lambda^n], \tag{7}$$

where $[T^n_\Lambda]$ is a transformation matrix between each elemental coordinate and is expressed as

$$\left[\ T^n_\Lambda\ \right] = \begin{bmatrix} T_{11} & T_{12} & T_{13} & \cdot & \cdot & \cdot & T_{1n} \\ & T_{22} & T_{23} & \cdot & \cdot & \cdot & T_{2n} \\ & & T_{33} & \cdot & \cdot & \cdot & T_{3n} \\ & & & \cdot & \cdot & \cdot & \cdot \\ & & & & \cdot & \cdot & \cdot \\ & 0 & & & & \cdot & \cdot \\ & & & & & & T_{nn} \end{bmatrix}. \tag{8}$$

$[T_{ij}](i,j=1\sim n)$ is expressed using matrix $[A_i]$ shown in (6b) as

$$[T_{ij}] = [A_i][A_j]^T. \tag{9}$$

$[\Lambda^n]$ is a matrix expressed as

$$\left[\ \Lambda^n\ \right] = \begin{bmatrix} \Lambda_1 & & & & & \\ & \Lambda_2 & & & 0 & \\ & & \Lambda_3 & & & \\ & & & \cdot & & \\ & & & & \cdot & \\ & 0 & & & \cdot & \\ & & & & & \Lambda_n \end{bmatrix}, \tag{10}$$

where

$$\left[\ \Lambda_i\ \right] = \begin{bmatrix} 0 & l_i & 0 & 1 & 0 & 0 \\ l_i & 0 & 0 & 0 & 1 & 0 \\ 0 & 0 & 0 & 0 & 0 & 1 \end{bmatrix}. \tag{11}$$

Consequently, joint torques can be obtained, as shown in (2), first by converting the nodal forces in global coordinates to elemental coordinates and next by multiplying the matrix regarding link lengths. The nodal forces are calculated by supplying accurate target motions that compensate for the inertial forces acting at the links. Therefore, a kinematics solution scheme using the finite element approach was also developed to handle the elasticity of the links. See the references [3], [7] and [8] for more details.

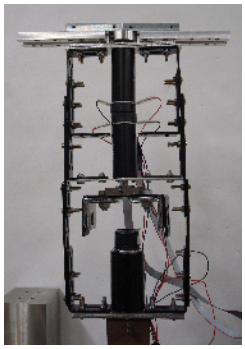

Fig. 4. Experimental setup of a rotor mechanism with uniaxial TCS mounted on the rotating axis.

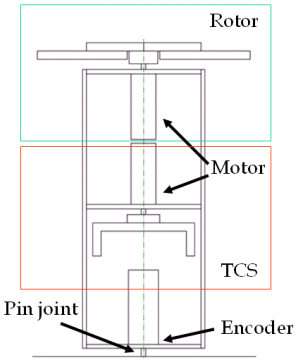

Fig. 5. Layout of a rotor and a TCS.

IV. Torque Cancelling Experiments

A. Rigid Rotor - Uniaxial TCS System

A simple rotor-TCS experimental setup, as shown in Figs. 4 and 5, was made to carry out a numerical estimation and some experiments for verification. In this setup, a rotor is driven by a gearless motor, and a prototype TCS is placed underneath, exactly on the rotating axis of the rotor. The frame body is connected to the ground with a rotation-free pin joint, where an encoder attached to a nonacutated motor is used to detect the rotational angle of the frame body. The rotor is made of aluminum, and the frame body is made of stainless steel, both with enough sectional area such that the whole architecture can be assumed to be rigid without any elastic deformation.

Figure 6 shows the finite element subdivision of the experimental setup, with each connection to connection modeled with a single Bernoulli-Euler beam element. The whole system is modeled with a total of 21 elements and 22 nodes. The capabilities of modeling this kind of complex architecture and computing the dynamics are the main features of the parallel solution scheme.

A rotational motion of 4π rad in 2 s is given to the rotor. The torque required for driving the rotor, which is actually computed at the upper node of element No. 3 in Fig. 6, is obtained by the parallel solution scheme as shown in Fig.

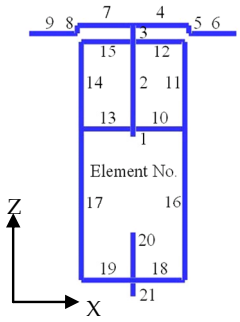

Fig. 6. Finite element subdivision of the setup.

7(a). Reaction moments generated at the exact location of the TCS (lower node of element No. 1 in Fig. 6) are calculated as shown in Fig. 7(b). To cancel these moments, the torque shown in Fig. 7(c) should be supplied to the TCS. Note that the cancelling torques the TCS has to generate are a perfect duplicate of the reaction moments (see Fig. 1).

Figure 8 shows the rotational angle of the frame body detected at the encoder attached on the pin joint when the

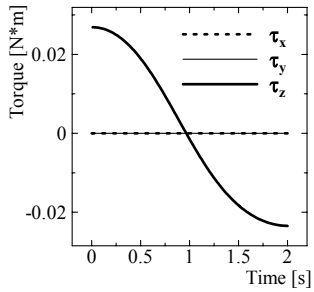

(a) Motion torque for driving the rotor.

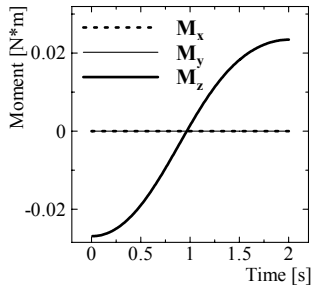

(b) Reaction moment generated at the exact location of TCS.

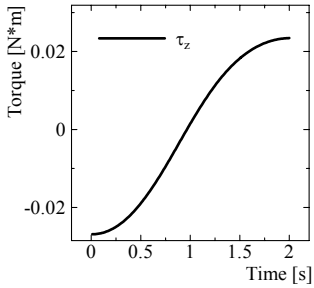

(c) Input torque for TCS.

Fig. 7. Input torques and generated moments in the system.

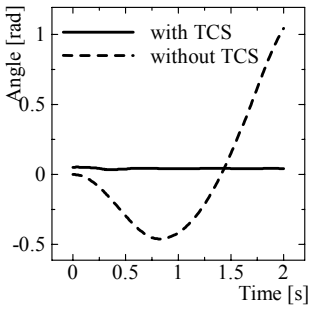

Fig. 8. Rotational angle of the frame body around the pin joint during the motion.

motion torque is actually supplied to the rotor. It can be confirmed from the figure that the frame body is unstable during the motion when the TCS is not activated, whereas the rotation around the pin joint stops perfectly when the TCS is activated, which means that the reaction moments generated around the rotating axis are cancelled perfectly by supplying the accurately computed cancelling torques to the TCS.

B. Rigid Rotor in Offset Position - Uniaxial TCS System

Next, an experiment was carried out on a different configuration of the frame body, as shown in Figs. 9 and 10. In this case, a TCS is mounted in the offset position of the rotating axis to see if such a condition affects the capability of the system. The whole system is modeled with a total of 25 elements and 26 nodes as shown in Fig. 11. The same rotational motion is given to the rotor as in the previous experiment, and, consequently, there is no difference between Fig. 7(a) and Fig. 12(a). The motion torques for driving the rotor are the values calculated at the upper node of element No. 3, and the reaction moments are the values calculated at the upper node of element No. 25. The reaction moment and the input torque for the TCS around the z axis in Figs. 12(b) and 12(c) perfectly agree with those in Figs. 7(b) and 7(c). On the other hand, M_y in Fig. 12(b) is constantly shifted to the positive direction because a moment due to gravity subjected along the offset length is now generated. The moment generated by gravity, however, is supported at the pin joint and is not meant to be suppressed in this

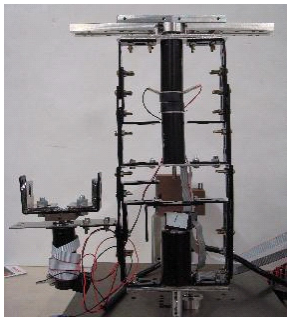

Fig. 9. Experimental setup of a rotor mechanism with uniaxial TCS mounted in the offset position of the rotating axis.

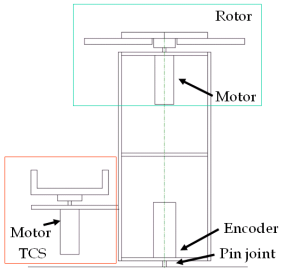

Fig. 10. Layout of a rotor and a TCS.

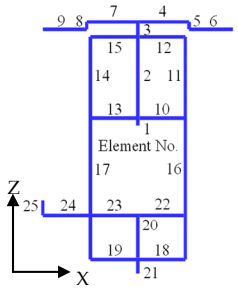

Fig. 11. Finite element subdivision of the setup.

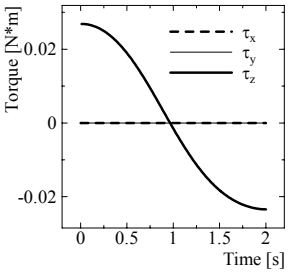

(a) Motion torque for driving the rotor.

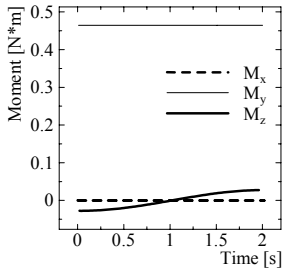

(b) Reaction moment generated at the exact location of TCS.

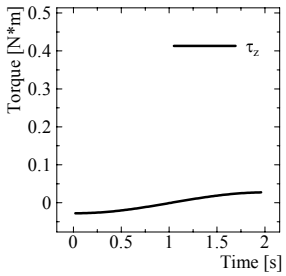

(c) Input torque for TCS.

Fig. 12. Input torques and generated moments in the system.

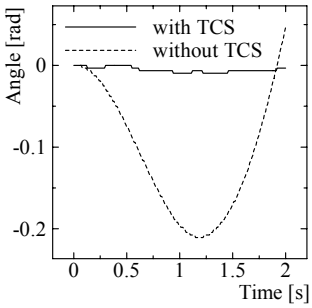

Fig. 13. Rotational angle of the frame body around the pin joint during the motion when a TCS is mounted in the offset position.

experiment.

It can be confirmed from Fig. 13 that also in this case, the mechanical sway around the pin joint is successfully suppressed to a minimal amount by activating the TCS mounted in the offset position.

C. *Flexible Link - Uniaxial TCS System*

Lastly, a simple flexible link with TCS experimental setup, as shown in Figs. 14 and 15, was made to carry out a numerical estimation and some experiments for verification. In this setup, a flexible link is driven by a gearless motor, and a prototype TCS is placed at an offset position from the rotating axis of the active joint. The link system is connected to the ground with a rotation-free passive joint, where an encoder attached to a nonacutated motor is used to detect the rotational angle of the overall body. The flexible link is made of poly-carbonate, where the elastic deformation occurred in the link should not be neglected in the inverse dynamics calculation. The experimental setup is subdivided, with each connection to connection by a single

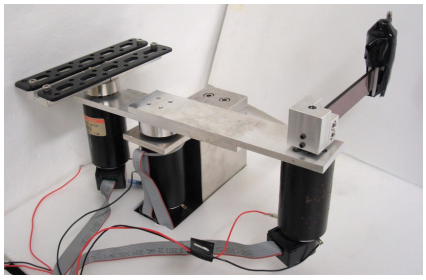

Fig. 14. Experimental setup with uniaxial TCS.

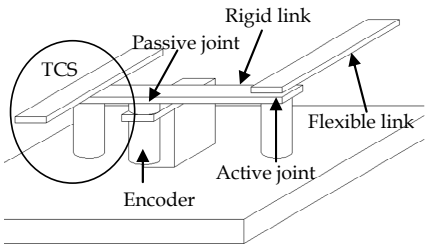

Fig. 15. Configuration of the setup and location of a TCS.

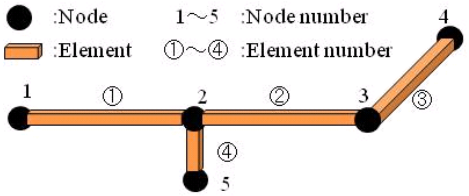

Fig. 16. Finite element subdivision of the setup.

Bernoulli-Euler beam element. The whole system is modeled with a total of 4 elements and 5 nodes as shown in Fig. 16. The capabilities of modeling this kind of architecture with flexible link and computing the dynamics are, again, the main features of the parallel solution scheme.

A rotational motion of π rad in 2 s is given to the active link. The torque required for the active joint is obtained by

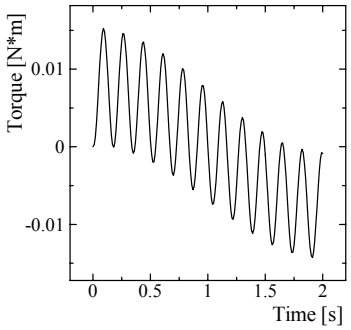

(a) Motion torque for driving the flexible link.

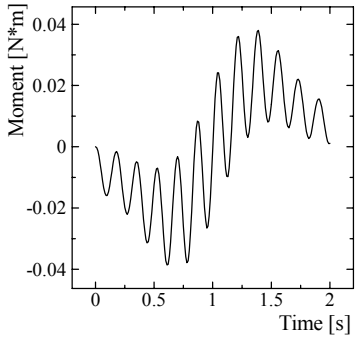

(b) Reaction moment generated at the exact location of TCS.

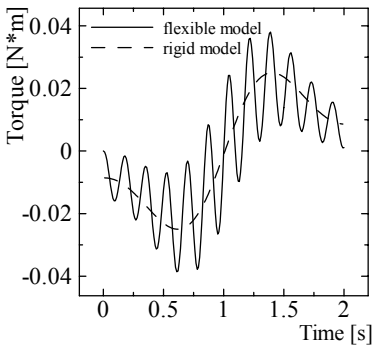

(c) Input torque for TCS.

Fig. 17. Input torques and generated moments in the system.

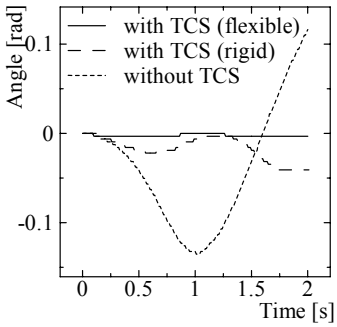

Fig. 18. Rotational angle of the link system around the passive joint during the motion.

the parallel solution scheme as shown in Fig. 17(a). Reaction moment generated at the exact location of the TCS is calculated as shown in Fig. 17(b). To cancel this moment, the torque shown in Fig. 17(c) should be supplied to the TCS. Here again, note that the cancelling torque the TCS has to generate is a perfect duplicate of the reaction moment (see Fig. 1). A torque curve for the TCS when the active link is assumed as a rigid member, without any elastic deformation, is also shown in the figure. This torque curve is also supplied to the TCS to see how the accurate consideration of dynamics is important in the torque cancelling.

Figure 18 shows the rotational angle of the link system detected at the encoder attached on the passive joint, when the motion torque is actually supplied to the active joint. It can be confirmed from the figure that the link system is unstable during the motion when the TCS is not activated, whereas the rotation around the passive joint stops perfectly when the TCS is activated (by the torque obtained by assuming the elasticity of the flexible link), which means that the vibrating reaction moment generated around the rotating axis are cancelled perfectly by supplying the accurately computed cancelling torque to the TCS. Also, it can be confirmed that the torque curve obtained by not assuming the elasticity of the flexible link, is not sufficient for the TCS to suppress the reaction moment generated around the passive joint.

V. Conclusion

The torque cancelling system proposed and developed in this paper succeeded to suppress a mechanical sway generated by the motions of rigid or flexible objects. The suppression was realized by considering the accurate dynamics of the objects and the main body itself using a newly developed calculation scheme of inverse dynamics. As a consequence, innovation of the finite element approach to the inverse dynamics calculation enables us to consider more precise dynamics of robots, which leads to more precise feedforward control and cancellation of mechanical sway during quick motions. Further simulations and experiments on triaxial cases are scheduled. Furthermore, we are developing a more compact TCS device that can be mounted on actual robots.

Acknowledgment

The author wishes to acknowledge the contributions of the following former and present graduate students of his laboratory: Takeo Ueda, Daisaku Imaizumi, Youichi Chikugo, Shunsuke Sato, Atsushi Yagi, Akihiro Kato, Koji Yamanaka, Hiromasa Ueda, Yuto Kitamura, and Junya Hayakawa.

References

[1] Y. Ookami, N. Tomita, S. Nakasu, and S. Matsunaga, "Introduction to the Space Station," University of Tokyo Press, 2008, pp. 204-208, in Japanese.

[2] K. Yoshida, D. N. Nenchev, and K. Hashizume, "Flight Experiments of ETS-VII for Advanced Space Robot Control," J. Society of Japanese Aerospace Companies, Vol. 50, No. 584, 2002, pp. 351–359, in Japanese.

[3] D. Isobe, "A Unified Solution Scheme for Inverse Dynamics," Advanced Robotics, Vol. 18, No. 9, 2004, pp. 859-880.

[4] Y. Nakamura, and M. Ghodoussi, "Dynamics Computation of Closed-Link Robot Mechanisms with Nonredundant and Redundant Actuators," IEEE Trans. Robotics and Automation, Vol. 5, No. 3, 1989, pp. 294-302.

[5] Y. Nakamura and K. Yamane, "Dynamics Computation of Structure-Varying Kinematic Chains and Its Application to Human Figures," IEEE Trans. Robotics and Automation, Vol. 16, No. 2, 2000, pp. 124-134.

[6] K. Sugimoto, "Dynamic Analysis of Closed Loop Mechanisms on the Basis Vectors of Passive Joint Axes," J. Robotic Systems, Vol. 20, No. 8, 2003, pp. 501-508.

[7] D. Isobe, A. Yagi, and S. Sato, "General-Purpose Expression of Structural Connectivity in the Parallel Solution Scheme and Its Application," JSME Int. J. Series C, Vol. 49, No. 3, 2006, pp. 789-798.

[8] D. Isobe, and A. Kato, "Feedforward Control of Flexible Link Systems using Parallel Solution Scheme," Int. J. Robotics and Automation, Vol.23, No.1, 2008, pp.31-39.